Oxygen-induced p(3×1) reconstruction of the W(100) surface

S. Murphy [1], G. Manai, I.V. Shvets

SFI Laboratory, Physics Department, Trinity College, Dublin 2, Ireland

Abstract

The oxidation of the W(100) surface at elevated temperatures has been studied using room temperature STM and LEED. High exposure of the clean surface to O_2 at 1500 K followed by flash-annealing to 2300 K in UHV results in the formation of a novel p(3 × 1) reconstruction, which is imaged by STM as a missing-row structure on the surface. Upon further annealing in UHV, this surface develops a floreted LEED pattern characteristic of twinned microdomains of monoclinic WO_x, while maintaining the p(3×1) missing-row structure. Atomically resolved STM images of this surface show a complex domain structure with single and double W⟨010⟩ rows coexisting on the surface in different domains.

Key words:
Scanning tunneling microscopy, tungsten, oxygen, reconstruction
PACS: 68.37.Ef, 68.47.De, 68.47.Gh

1 Introduction

The W(100) surface has been extensively studied with respect to the range of reconstructions observed on both the clean and adsorbate-covered surfaces [1–4]. The interaction of oxygen with the W(100) surface has been particularly well-studied. At room temperature the surface transforms with increasing oxygen exposure, giving rise to a p(4×1) → c(8×2) → p(8×1) → p(4×1) → p(2×2) series of low-energy electron diffraction (LEED) patterns, while at elevated temperatures (∼ 1050 K), the surface undergoes a p(2×1) → p(5×1) → IC(5×1) → p(2×2) → (1×1) series of transformations, where the incommensurate (IC) (5×1) structure comprises a mixture of (5×1) and (4×1) structures

[1] Corresponding Author. Fax: + 353 1 608 3228; e-mail: shmurphy@tcd.ie

[5,6]. The high-temperature p(2×1) and p(5×1) reconstructions are attributed to missing-row structures aligned along the orthogonal ⟨100⟩ and ⟨010⟩ directions, where the oxygen atoms are incorporated at threefold hollow sites on the {011} type facets formed between the first and second layer W atoms [6,7]. The missing-row structure has been resolved by scanning tunneling microscopy (STM) in the case of the p(2×1) reconstruction [8]. It was found that excess oxygen resulted in the multilayer growth of W⟨100⟩ and W⟨010⟩ non-missing rows, which provide additional binding sites for the oxygen.

The above reconstructions are formed at low exposures (≤4–7 Langmuir) and are precursors to tungsten oxide formation. Tungsten trioxide WO_3 is the most stable oxide of tungsten and the final product of the oxidation of a tungsten surface. It is of particular interest due to its technological applications in electrochromic devices and chemiresistive gas sensors [9,10]. The WO_3 structure is based on corner-sharing WO_6 octahedra and resembles the cubic crystal structure of ReO_3. However, at room temperature (γ-)WO_3 has a monoclinic distortion, giving it cell parameters of a = 7.297 Å, b = 7.539 Å, c = 7.688 Å and $\beta = 90.91°$. At elevated temperatures (T > 600 K), it undergoes a transition to an orthorhombic phase. While pure stoichiometric WO_3 has a bandgap of 2.6 eV, it is possible by reducing the crystal to perform STM and LEED on single crystal and thin film surfaces [11–16]. Tungsten dioxide WO_2 is another important oxide of tungsten, which displays room temperature metallic conductivity. It is based on a distorted tetragonal rutile structure. The distortion comes from pairing of W ions in chains of edge-sharing WO_6 octahedra along the crystallographic a-axis, resulting in a monoclinic cell with cell parameters of a = 5.563 Å, b = 4.896 Å, c = 5.663 Å and $\beta = 120.47°$ [17].

In this study, we present details of a STM and LEED study of the oxidation of the W(100) surface at elevated temperatures. We report the formation of a novel p(3×1) missing-row reconstruction. While a (3×1) or (3×3) reconstruction has previously been reported during oxidation of the W(100) surface [5], it is not so commonly observed as on the closely similar Mo(100) and Ta(100) surfaces [18–20]. During oxidation of the Mo(112) surface, p(2×3) and p(1×3) missing-row reconstructions have been identified as precursors to the formation of an epitaxial MO_2 layer [21–23]. In the present case, the nucleation of a penetrated oxide WO_x is also observed at the boundaries between orthogonal domains of the p(3×1) reconstruction.

2 Experimental

The sample preparation and analysis were performed in an ultra-high vacuum (UHV) system with a base pressure in the low 10^{-10} Torr, which was equipped for room-temperature STM, LEED and Auger electron spectroscopy

(AES). The substrate was prepared from a 5N purity W single crystal, which was aligned to within $\pm 0.5^\circ$ of the (100) crystal plane and mechanically polished to a surface roughness of 0.01 μm. To remove carbon and other impurities from the surface, the sample was heated by electron-bombardment to $1600 \leq T \leq 1900$ K in an O_2 partial pressure of 1×10^{-6} Torr for periods of 30-60 minutes. After each of these anneals, the substrate was then flash-annealed several times to 2500 K for 10-15 second intervals under UHV conditions. Once carbon was removed from the surface, the sample was cleaned by flash-annealing to remove the oxygen. The sample temperature was monitored using an infra-red pyrometer (Ircon, Ultimax UX-20P) with an emissivity value of 0.35 at 1 μm wavelength. We estimate the accuracy of the temperature measurements to be within ± 100 K. The STM images presented here were obtained at room temperature in constant current mode using MnNi tips [24], with the sample biased with respect to the tip.

3 Results and discussion

The clean surface displayed a sharp 1×1 LEED pattern, like that shown in Fig. 1(a). STM images of this surface displayed atomic terraces, varying in width from the order of 100 Å to 2000 Å, which were separated by monatomic steps 1.6 ± 0.2 Å in height. More details of STM experiments on W(100) are given elsewhere [25]. The p(3×1) LEED pattern shown in Fig. 1(b) could be obtained by annealing the surface for several hours at 1500 ± 100 K in an O_2 partial pressure of 1×10^{-6} Torr and subsequently flash-annealing the surface to 2300 ± 100 K until a reasonably sharp LEED pattern was achieved. A periodicity of 9.4 ± 0.4 Å was estimated for the reconstruction from this LEED pattern. Further annealing of this surface in UHV leads to the formation of the floreted LEED pattern shown in Fig. 1(c). In this case, both the integral- and fractional-order spots are split along the [001] and [010] directions. An important feature of this splitting is that it is largely independent of the primary electron beam energy and does not display the oscillatory behaviour with energy expected for a highly stepped surface [26]. Rather, this is analagous to the LEED pattern formed by twinned monoclinic microdomains on WO_3 single crystal surfaces [11,13]. Because of the noncubic unit cell, the normal vectors of adjacent domains are tilted with respect to each other by an angle $2(\beta\text{-}90)^\circ$. The spot-splitting results from the superposition of the diffraction patterns from adjacent domains, which have slightly different incident beam angles. This has been confirmed by the disappearance of the spot-splitting when the sample is held at a temperature above the monoclinic to orthorhombic phase transition for WO_3 [15]. From the spot-splitting in Fig. 1(c), the angle $2(\beta\text{-}90)^\circ$ is estimated as $3.2 \pm 0.5^\circ$, giving a monoclinic angle of $\beta = 91.6 \pm 0.3^\circ$. This is in good agreement with the value obtained on WO_3 single crystal sur-

faces [11,13]. We conclude that annealing the oxidised W(100) surface in UHV, reduces the oxide to a monoclinic phase close to WO_3. STM images show that the oxide layer is not homogeneous on the surface.

Figure 2(a) shows a large-scale STM image of the surface corresponding to the LEED pattern shown in Fig. 1(b). The surface appears to be more heavily oxidised in some areas than in others. Atomic terraces are visible on some areas of the surface, as shown in Fig. 2(b). The minimum step height measured between successive terraces is 1.6 ± 0.2 Å. Higher resolution images taken on these terraces resolve orthogonal domains of the p(3×1) missing-row reconstruction. The lateral dimension of the domains is typically of the order of 5–50 nm and antiphase domain boundaries are observed. An antiphase boundary is shown in Fig. 2(c), where the W⟨001⟩ rows in two adjacent parallel domains are shifted with respect to one another by one lattice spacing (~ 3 Å) along the [010] direction. Figure 3 (a) shows a large-scale STM image taken of the surface corresponding to the floreted LEED pattern shown in Fig. 1(c). The atomic terraces appear to be larger on average, but higher resolution images, *c.f.* Fig. 3 (b), show them to be comprised of similar sized p(3×1) reconstruction domains as those shown in Fig. 2. It should be noted at this point, that while the domain size in both Figs. 2 and 3 is comparable to the *transfer width* of the LEED optics (typically ~ 10 nm) [27], the spot-splitting is only observed in the latter case. The domains shown in Fig. 3(b) are distinguished by the presence of protrusions at the domain boundaries. This is shown more clearly in Fig. 3(c), where the decoration of the boundary between two domains is resolved. The periodicity of the protrusions along the [001] direction matches that of the reconstruction, which may explain the splitting of the fractional-order spots in the LEED pattern. The height of these protrusions varies from ~ 1 Å to ~ 4 Å when measured at different points on the surface. They are attributed to the formation of a penetrated oxide WO_x at the domain boundaries. This agrees well with low-energy electron microscopy (LEEM) observations of oxide formation on the p(5×1) reconstructed W(100) surface [6], where it was observed that the oxide nucleation begins by decoration of the domain walls of the reconstruction, giving rise to oxide nuclei chains on the surface.

Figure 4 shows atomically resolved STM images of the two types of p(3×1) missing-row structure found on the surface. The structures in Figs. 4(a) and (b) were observed in different domains on the surface shown in Fig. 3. It is assumed that W atoms are imaged at the surface, though STM studies of the WO_3(001) surface suggest that oxygen atoms may alternatively be resolved [12,13]. In both cases, the average periodicity measured along the [010] direction is 3.0 ± 0.1 Å, while the average periodicity measured along the orthogonal [001] direction is 9.0 ± 0.3 Å. These values correspond well to the interatomic periodicity of the W(100) surface (3.165 Å) and do not match the periodicities expected for either the bulk WO_2 or WO_3 (100) surfaces [12,17].

The tunnel bias used to obtain the STM images in Fig. 4 is typical of that used to image metal surfaces. By comparison, the tunnel bias used to obtain atomically resolved images on WO_3 single crystal and 40–100 nm thin film surfaces is typically in the 1.5–2.0 V range [14–16]. This suggests that the structures imaged in Fig. 4 are localised to the surface and do not represent penetrated oxides.

The proposed model for each of the observed missing-row structures is also displayed in Fig. 4. The models are based on those proposed for the p(2×1) and p(5×1) missing-row reconstructions [6–8], since the observed structures appear to agree very well with the latter. Figure 4(e), representing the STM image in Fig. 4(a), comprises double W⟨010⟩ rows separated by a missing W row. Oxygen atoms bind to the quasi-threefold sites situated on the (101) facets formed at the missing rows and in the four-fold hollow sites on the non-missing rows. In terms of oxygen coverage, the structure shown in Fig. 4(e) is equal to 1.0 ML, where one monolayer (ML) equals 9.98×10^{18} atoms m^{-2}, which is the atomic packing density of the W(100) plane. However, if instead of occupying the four-fold hollow sites, oxygen atoms occupy positions on top of the non-missing W rows, the corresponding coverage increases to 1.3 ML. Figure 4(f), corresponding to the STM image shown in Fig. 4(b), represents a multilayer reconstruction where an additional W⟨010⟩ is present on top of the double rows shown in Fig. 4(a), (e), thereby increasing the number of three-fold sites available to bind oxygen atoms [8]. This structure also corresponds to a coverage of 1.0 ML, but can also increased to 1.3 ML if oxygen atoms in on-top positions are assumed. Both of these structures are possible precursors to the (4×1) and (5×1) structures discussed in reference [6].

To experimentally determine the oxygen coverage associated with the p(3×1) reconstruction, the O/W AES signal ratio was measured and compared with that for the well-known p(2×1) reconstruction [8]. For the AES measurements, the p(3×1) reconstruction was reproduced by annealing the clean surface in 5×10^{-7} Torr of O_2 at 1400 ± 100 K for one hour. A LEED pattern of this structure is shown in Fig. 5(a). The p(2×1) structure shown in Fig. 5(b) was obtained by dosing the clean surface with 1×10^{-8} Torr of O_2 for 2-7 min at 300 K, followed by annealing at 1400 K for 5-8 min. Assuming a coverage of 0.5 ML for the p(2×1) reconstruction [8], a comparison of the O/W AES signal ratios for the p(2×1) and p(3×1) reconstructions indicates that the p(3×1) structure corresponds to an oxygen coverage of approximately 1.0-1.5 ML. This is in good agreement with the value predicted from the models presented in Fig. 4.

4 Conclusions

To summarise, high-temperature oxidation and annealing of the W(100) surface results in the formation of a novel p(3×1) reconstruction. Atomically resolved STM images of this reconstruction reveal it to be a missing-row structure with two possible configurations, comprising either single or double W⟨010⟩ non-missing rows. The associated oxygen coverage estimated from structure models and Auger measurements places this structure in the coverage range between the previously observed p(2×1) and p(5×1) high-temperature reconstructions. Nucleation of a penetrated oxide WO_x is also observed to occur at the domain boundaries, in agreement with previous studies of W(100) oxidation.

5 Acknowledgments

This work was supported by the Science Foundation Ireland agency under contract 00/PI.1/C042.

References

[1] P.J. Estrup, Surf. Sci. 299-300 (1994) 722.

[2] P.F. Lyman, D.R. Mullins, Phys. Rev. B 51 (1995) 13623.

[3] Ch. Park, H.M. Kramer, E. Bauer, Surf. Sci. 115 (1982) 1.

[4] C. Park, H.M. Kramer, E. Bauer, Surf. Sci. 116 (1982) 467.

[5] E. Bauer, H. Poppa, Y. Viswanath, Surf. Sci. 58 (1976) 517.

[6] M.S. Altman, E. Bauer, Surf. Sci. 347 (1996) 265.

[7] H. Yamazaki, T. Kamisawa, T. Kokubun, T.Haga, S. Kamimizu, S. Sakamoto, Surf. Sci. 477 (2001) 174.

[8] J.A. Meyer, Y. Kuk, P.J. Estrup, P.J. Silverman, Phys. Rev. B 44 (1991) 9104.

[9] C.G. Granqvist, Solar Energy Mater. Solar Cells 60 (2000) 201.

[10] S.C. Moulzolf, L.J. LeGore, R.J. Lad, Thin Solid Films 400 (2001) 56.

[11] M.A. Langell, S.L. Bernasek, J. Vac. Sci. Technol. 17 (1980) 1296.

[12] F.H. Jones, K. Rawlings, J.S. Foord, P.A. Cox, R.G. Egdell, J.B. Pethica, B.M.R. Wanklyn, Phys. Rev. B 52 (1995) R14392.

[13] F.H. Jones, K. Rawlings, J.S. Foord, R.G. Egdell, J.B. Pethica, B.M.R. Wanklyn, S.C. Parker, P.M. Oliver, Surf. Sci. 359 (1996) 107.

[14] F.H. Jones, R.A. Dixon, A. Brown, Surf. Sci. 369 (1996) 343.

[15] R.E. Tanner, E.I. Altman, J. Vac. Sci. Technol. A 19 (2001) 1502.

[16] M. Li, E.I. Altman, A. Posadas, C.H. Ahn, Surf. Sci. 542 (2003) 22.

[17] F.H. Jones, R.G. Egdell, A. Brown, F.R. Wondre, Surf. Sci. 374 (1997) 80.

[18] R. Riwan, C. Guillot, J. Paigne, Surf. Sci. 47 (1975) 183.

[19] E. Bauer, H. Poppa, Surf. Sci. 88 (1979) 31.

[20] A.V. Titov, H. Jagodzinski, Surf. Sci. 152-153 (1985) 409.

[21] T. Schroeder, J.B. Giorgi, A. Hammoudeh, N. Magg, M. Baümer, H.-J. Freund, Phys. Rev. B (2002) 115411.

[22] A.K. Santra, B.K. Min, D.W. Goodman, Surf. Sci. 513 (2002) L441.

[23] T. Schroeder, J. Zegenhagen, N. Magg, B. Immaraporn, H.-J. Freund, Surf. Sci. 552 (2004) 85.

[24] S.F. Ceballos, G. Mariotto, S. Murphy, I.V. Shvets, Surf. Sci. 523 (2003) 131.

[25] H. Wengelnik, D. Badt, H. Neddermeyer, Surf. Sci. 307-309 (1994) 619.

[26] M. Henzler, Surf. Sci. 73 (1978) 240.

[27] G. Comsa, Surf. Sci. 81 (1979) 57.

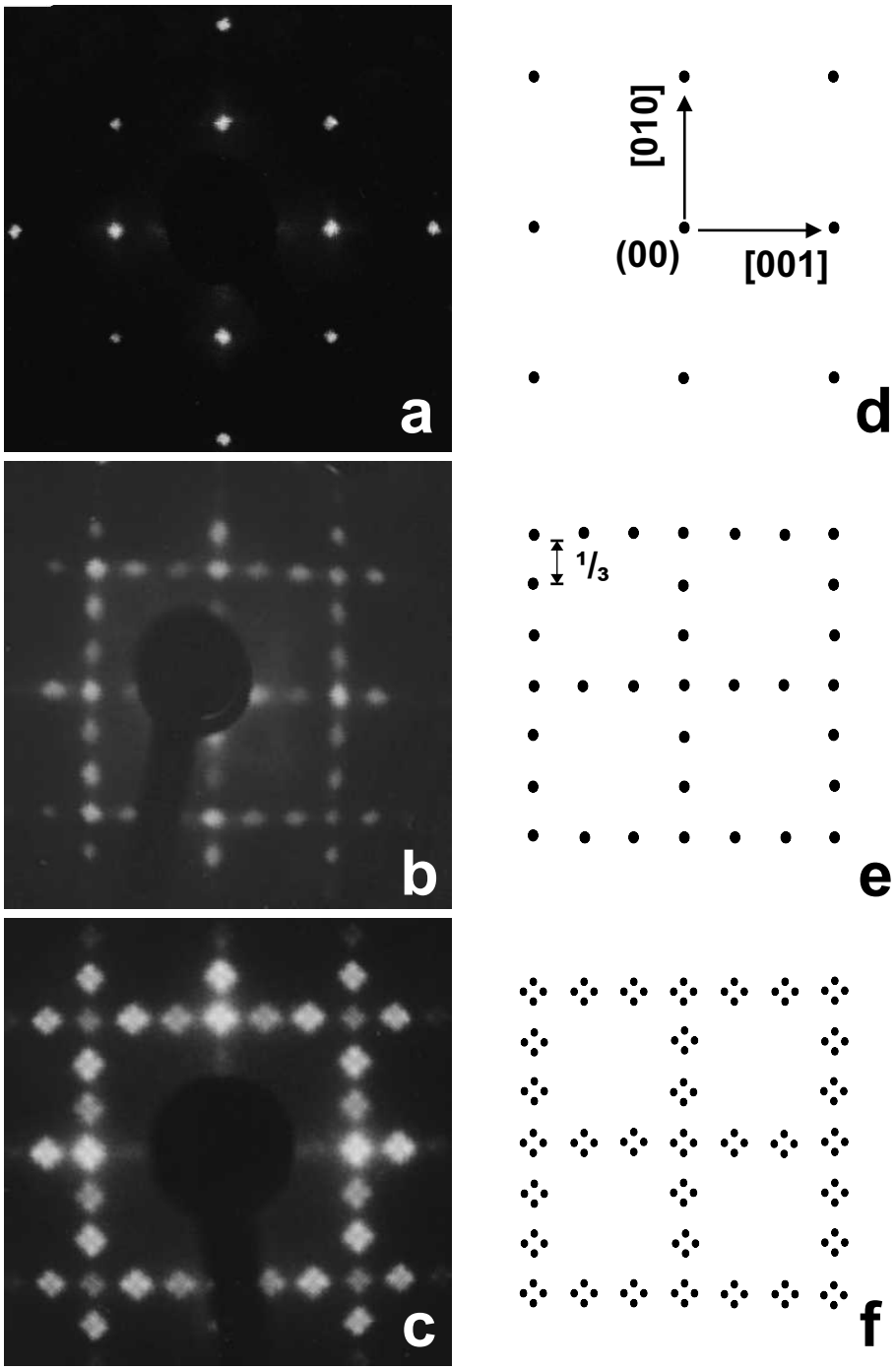

Fig. 1. (a) LEED pattern of the clean W(100) surface taken at 159 eV. (b) LEED pattern taken at 106 eV of the p(3×1) reconstructed surface obtained by oxidising the clean surface. (c) The floreting of both integral and fractional-order spots in this LEED pattern taken at 99 eV suggests the formation of monoclinic WO_3-like domains on the surface. (d-f) The corresponding schematic representations of the LEED patterns shown in (a-c).

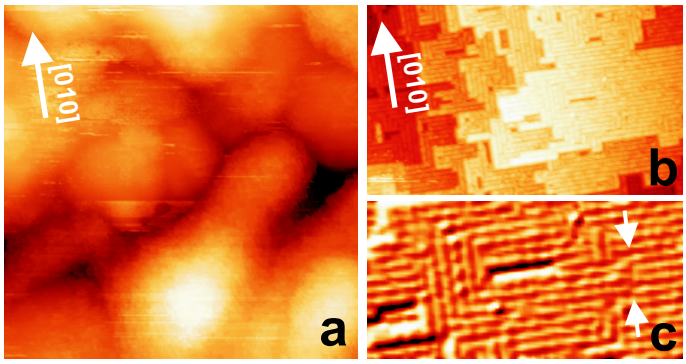

Fig. 2. (a) 500 nm × 500 nm STM image of the oxidised W(100) surface. (b) 59 nm × 36 nm image showing the atomic terraces found on areas of the surface. (c) 24 nm × 12 nm differentiated STM image of the upper terrace shown in image (b). Orthogonal rows of the p(3×1) reconstruction can be seen. Arrows indicate the position of an antiphase boundary between two parallel domains of the missing-row structure, where the W⟨001⟩ rows are shifted relative to one another along the [010] direction.

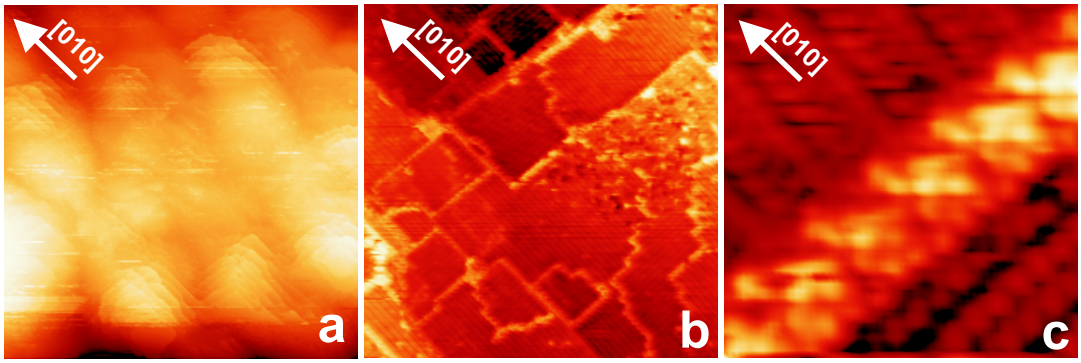

Fig. 3. (a) 500 nm × 500 nm STM image of the oxidised W(100) surface after annealing in UHV, which leads to the floreted LEED pattern. (b) 60 nm × 60 nm image of the surface, showing the decoration of the domain boundaries by WO_x protrusions. (c) 4 nm × 4 nm high-resolution image of the WO_x protrusions formed at the boundary between two orthogonal domains.

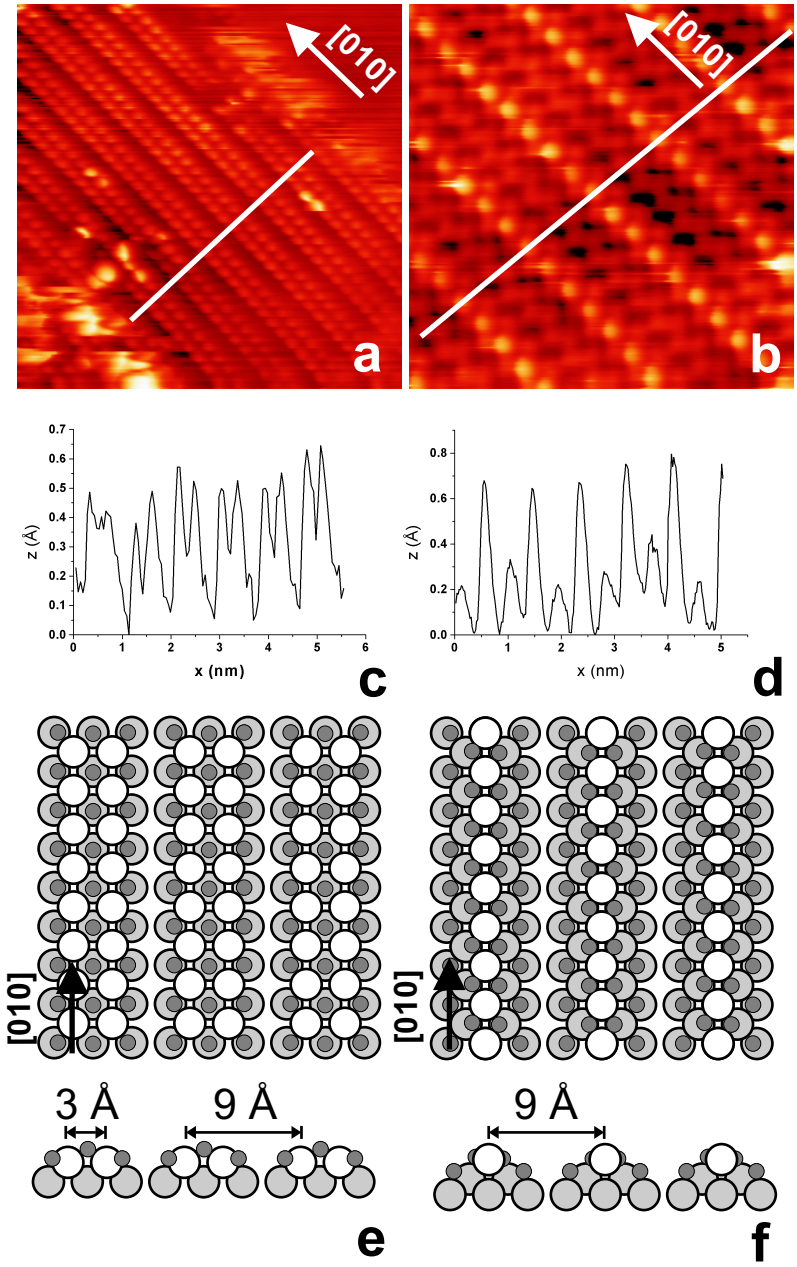

Fig. 4. (a, b) Atomically resolved STM images of different missing-row structures observed on the p(3×1) reconstructed W(100) surface. (a) 9 nm × 9 nm, I = 0.1 nA, V = 6 mV, (b) 4 nm × 4 nm, I = 0.3 nA, V = 10 mV and (c, d) line profiles taken along the directions marked in (a) and (b) respectively. (e, f) The corresponding models for each of these atomic images. The models are presented in both top and cross-sectional views. Open circles represent top-layer W atoms, grey circles represent W atoms in underlying layers, while the smaller dark circles represent oxygen bonded to the surface.

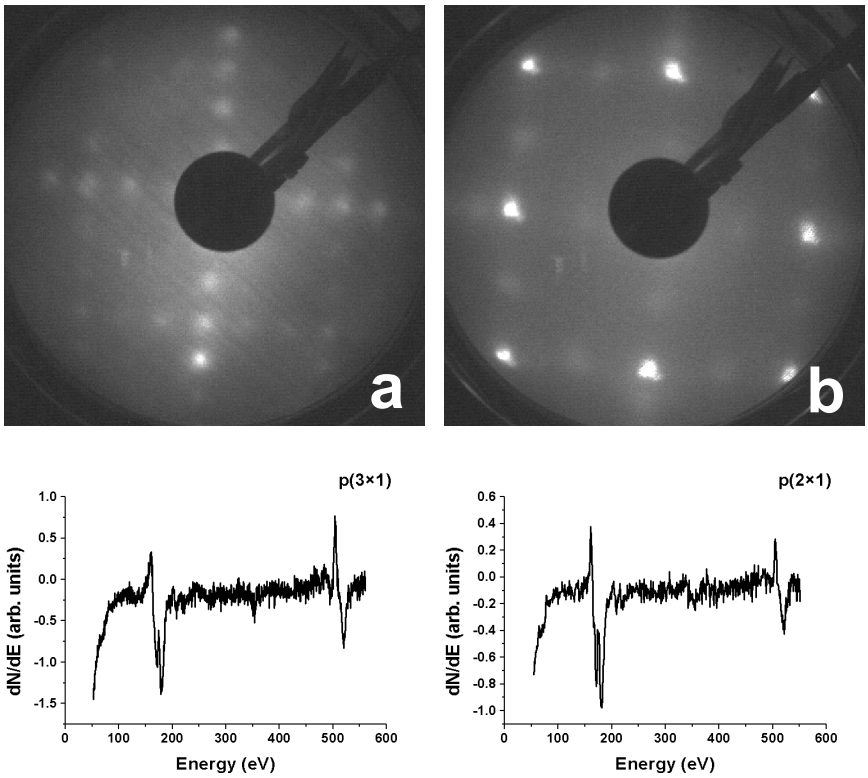

Fig. 5. (a) p(3×1) LEED pattern obtained by annealing the clean W(100) surface at 1400 K in 5×10^{-7} Torr of O_2 for one hour. Taken at 84 eV. (b) p(2×1) LEED pattern obtained by dosing the clean surface with 1×10^{-8} Torr of O_2 for 2-7 min at 300 K, followed by annealing at 1400 K for 5-8 min. Taken at 60 eV. Each LEED pattern is accompanied by the corresponding Auger spectrum in the 50-550 eV range.